journal

J. Am. Ceram. Soc., **88** [8] 2227–2229 (2005)
DOI: 10.1111/j.1551-2916.2005.00420.x

Mechanical Properties of Zirconia Thin Films Deposited by Filtered Cathodic Vacuum Arc

Zhenghao Gan†, Guoqing Yu, Zhiwei Zhao, C. M. Tan, and B. K. Tay

School of Electrical and Electronic Engineering, Nanyang Technological University, Singapore 639798, Singapore

Surface Young's modulus (*E*), hardness (*H*), and yield strength (*Y*) of zirconia films deposited on Si substrate by filtered cathodic vacuum arc (FCVA) under different oxygen flow rate were studied by nano-indentation measurement and finite element modeling. Identified by X-ray diffraction, the structure of the films evolves from amorphous to monoclinic, and then to amorphous, with oxygen flow rate increasing from 10 to 80 standard cubic centimeters per minute, which affects the mechanical properties of the films. It is found that the elastic–perfect-plastic constitutive model is successfully applied to the films with amorphous structure; however inadequate for the monoclinic ZrO_2, indicating that dislocation-related plasticity possibly occurs during nano-indentation.

I. Introduction

Zirconium oxide (ZrO_2) is a refractory material with excellent chemical and corrosion resistance and low thermal conductivity. Zirconia also has high hardness, making it a potential wear coating.[1] It is well known that brittle materials such as zirconia are subject to plastic deformation under mechanical contact, where the amount of elastic deformation is comparable with that of plastic deformation.[2] It is also known that experimental method itself such as nanoindentation is hard to predict the complex interaction in the vicinity of the contact zone between two contact materials. To study the plastic deformation of brittle materials such as zirconia, a constitutive relationship should be built. However, the conventional uniaxial tensile test at room temperature does not give a yield strength (Y) of zirconia since it is more likely to fail by fracture rather than plasticity under uniaxial tensile test.

Nanoindentation is a well-established technique for measuring films' mechanical properties. Both Young's modulus (E) and hardness (H) of the thin films are readily obtained by analyzing the detailed shape of the unloading curve during nanoindentation.[3] However, the report on yield strength of ZrO_2 thin film is limited since it could not be derived directly from the unloading curve of the nano-indentation measurement. For a metallic material under conditions of fully plastic indent, the yield strength is believed to be 1/3 of the hardness.[4] However, in ceramic materials like ZrO_2, yield occurs by bond cleavage, and the above relationship does not apply. The H/Y value is always lower than 3.[5]

Under nanoindentation, high hydrostatic stress level is around the contact zone, and an equivalent yield strength (EYS) could be defined to replace the usual yield strength given by the uniaxial test. In this work, with the aid of finite element simulation, the EYS of zirconia films are studied, which were deposited on Si (100) by filtered cathodic vacuum arc (FCVA)[6]. With the EYS at hand, the in-progress deformation of zirconia thin film under wear or mechanical contact is easy to be evaluated.

II. Experimental Details

The ZrO_2 thin films were deposited using an industrial FCVA system (Nanofilm Technologies International Pte Ltd, Singapore) described elsewhere.[7] The substrates were Si (100) with 400 μm average thickness, which were pre-cleaned with acetone, alcohol, and de-ionized water followed by a nitrogen blow-dry using a static neutralizing blow-off gun. Prior to deposition, the substrates were sputter cleaned for 2 min by argon ion beams (800 eV and 45 mA), and then transferred into the deposition chamber, which was evacuated to 2.0×10^{-6} Torr. A Zr cathode (99.98% pure) operated at 120 A DC current was ignited through instant contact between cathode and anode to obtain the plasma, which was steered out by a toroidal magnetic field fixed at 40 mT to condense on a substrate. O_2 gas (99.99%) was led into the region near the Zr target. O_2 flow rate chosen here was varied from 10 to 80 standard cubic centimeters per minute (sccm).

The nano-indentation measurement was performed by using Hysitron TriboScope (Hysitron Inc., Minneapolis, MN). In a typical indentation process, the Berkovich indenter was forced into a specimen using a pre-defined test force (400 μN), and a load/unload curve was recorded for each indentation. For each specimen, three independent indentations were performed. The experimental load/unload curve will be compared with that obtained from finite element modeling to derive the mechanical properties (E, Y, and H) of the thin films. The nominal thickness of the thin films is 500 nm.

The phases of the thin films were identified by XRD (X-ray diffractometer, D5005, Siemens, Madison, WI) using Cu$K\alpha$ radiation (wavelength of 1.54 Å) at 40 kV and 40 mA with a thin film goniometer (Rigaku, Tokyo, Japan). The incident angle of the X-ray is 1°.

III. Finite Element Approach

Some assumptions are made as follows to simplify the simulation: (1) The root-mean-square (RMS) roughness of the surface of the thin films is less than 0.1 nm. Thus, the surface roughness is ignored in the model; (2) Residual stress (i.e., pre-existing stress after deposition) is not included in the model; (3) Silicon substrate and ZrO_2 are assumed to be isotropic and behave as elastic perfect plastic. That is, only two parameters (i.e., E and Y) are needed to decide the constitutive model. This is a good approximation widely accepted[8–10] since they are brittle materials, where yield usually happens by bond cleavage and work hardening is not usually observed. The diamond indenter is assumed to be isotropic and to deform purely elastically, with $E = 1140$ GPa and $\nu = 0.07$;[11] (4) The friction between the indenter and the specimen under test is ignored; (5) Film-substrate is assumed to be mechanically bonded perfectly.

The indentation with a Berkovich indenter was modeled as a two-dimensional axisymmetric contact problem. This in one way could save a lot of computational time and in another

D. Marshall—contributing editor

Manuscript No. 10733. Received December 14, 2003; approved February 14, 2005.
†Author to whom correspondence should be addressed. e-mail: ezhgan@ntu.edu.sg

way produce a reasonable result.[8] Finite element package ANSYS (version 5.6) was employed for the indenter-specimen contact analysis in this work. The proposed finite element model was verified by employing nano-indentation measurement on the standard bulk fused silica provided by Hysitron® (Minneapolis, MN).[11] A detailed verification process was elaborated elsewhere.[12]

IV. Results and Discussion

(1) Structure of the Thin Films

The XRD patterns for ZrO_2 films deposited at different O_2 flow rate are shown in Fig. 1. Amorphous structure is observed at 10 sccm (Fig. 1(a)), indicated by a wide peak centered at $2\theta = 32.4°$, which is related to the oxygen-deficient Zr–O solid solution.[6] As O_2 flow rate increases to 20 sccm (Fig. 1(b)), one strong peak at $2\theta = 33.7°$ corresponds to (200) plane of monoclinic ZrO_2 (denoted as m(200)), accompanied by appearance of other weak peaks from monoclinic phase. At 35 sccm, in addition to more weak peaks, m(200) peak becomes weak while m(−202) peak gets strong. At 50 sccm, the strongest peak is m(−111) and more monoclinic peaks present. However, when O_2 flow rate rises to 65 sccm or above, the film transforms from polycrystalline into amorphous structure, evidenced by a wide peak at $2\theta = 31.3°$ (Fig. 1(e)). It is seen that the structure of the zirconia thin films evolves from amorphous through monoclinic to amorphous, with the increase of O_2 flow rate

(2) Mechanical Properties Versus Oxygen Flow Rate

Figures 2(a)–(c) shows the experimental loading–unloading curves and their simulation fittings for O_2 flow rate of 20, 50, and 80 sccm, respectively. In Figs 2(a) and (c), the simulation shows excellent agreement with the experimental results for both loading and unloading curves. However, for O_2 flow rate of 50 sccm (Fig. 2(b)), one may see the discrepancy in the latter part of the unloading curves: the experimental residual plastic deformation is much less than that of simulation, which may be attributed to the indentation-induced dislocation activity in ZrO_2 crystalline, as reported by Li *et al.*[13] Dislocation activity typically leads to plastic deformation, and thus the work hardening effect.

A qualitative explanation is given here for the larger predicted plasticity in the modeling (Fig. 2(b)). Figure 3 is a schematic comparison of the two hypothetical constitutive models of plastic (case 1) and perfect plastic (case 2). Note that work hardening is not included in case 2 (i.e., tangent modulus $E_1' = 0$), but be included in case 1 (i.e. $E_1' > 0$). W_1 and W_2 are the total works of indentation of cases 1 and 2, respectively. Subscripts e and p denote elastic and plastic portion, respectively. The total work of indentation should be equal for the two hypothetical cases

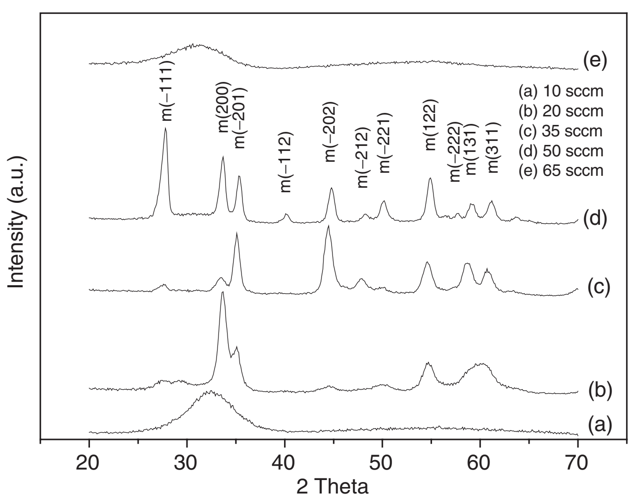

Fig. 1. X-ray diffraction patterns for the ZrO_2 films deposited at different O_2 flow rate.

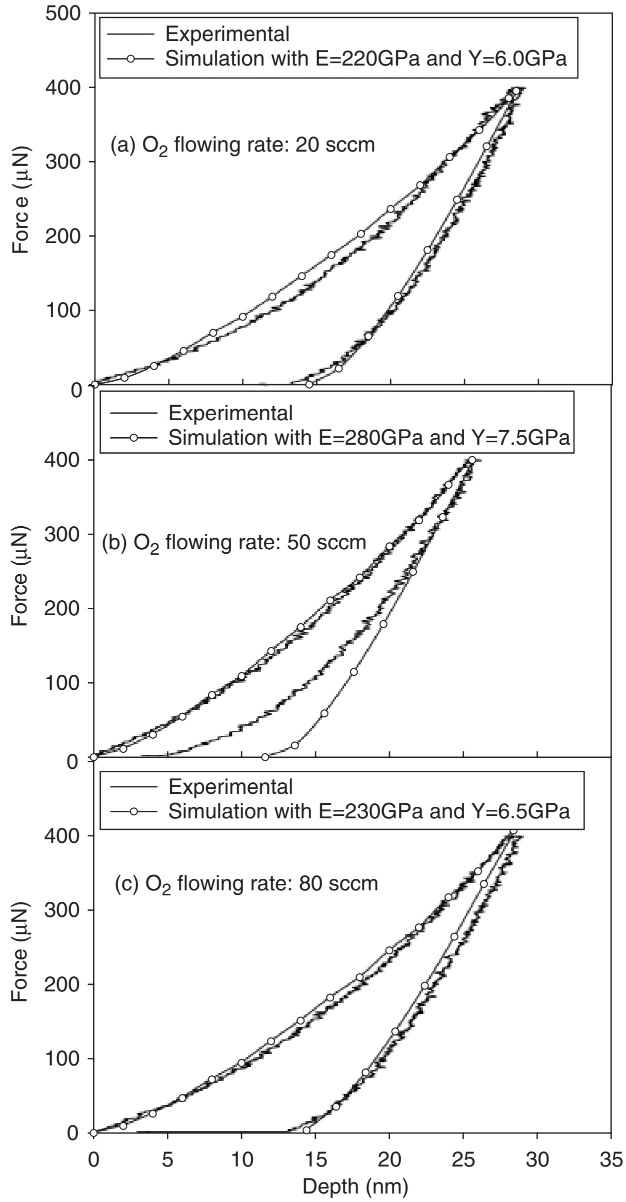

Fig. 2. Experimental loading-unloading curves and their simulation fittings for oxygen flow rate of: (a) 20; (b) 50, and (c) 80 sccm.

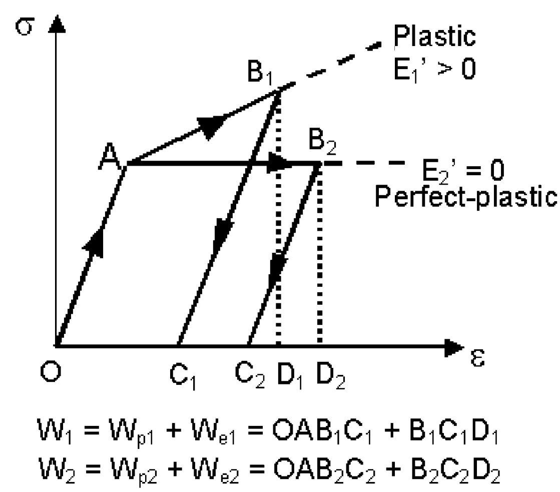

Fig. 3. Schematic constitutive models for plastic (case 1) and perfect plastic (case 2). W_1 and W_2 are the total works of indentation of cases 1 and 2, respectively. Subscripts e and p denote elastic and plastic portion, respectively. It is clear that the residual strain in case 2 (OC_2) is larger than that in case 1 (OC_1).

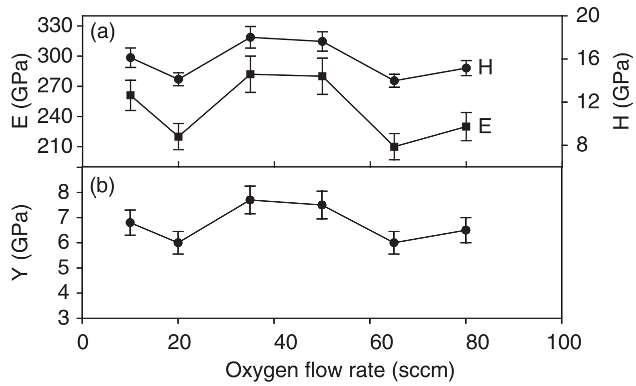

Fig. 4. (a) Young's modulus and hardness and (b) yield strength of the ZrO_2 thin films vary with the O_2 flow rate.

(i.e., $W_1 = W_2$), which is also equal to the experimental one. However, it is seen in Fig. 3 that the elastic recovery $W_{e1} > W_{e2}$ because of work hardening (i.e., area $B_1C_1D_1 > B_2C_2D_2$). Therefore, the residual plastic strain for perfect plastic (OC_2) is larger than that for plastic model (OC_1). In other words, the elastic–perfect plastic model assumed for the amorphous structure of the thin films (Figs. 2(a) and (c)) would be inappropriate for the monoclinic ZrO_2 (Fig. 2(b)).

Figure 4 presents the *E*, *Y*, and *H* of the zirconia thin films, exhibiting the same trend as the O_2 flow rate increases. The values of the properties are the largest in the middle gas flow region (i.e., in-between 35 and 50 sccm), which is corresponding to the monoclinic ZrO_2. The future work will be intended to study the structure variations controlling the changes in yield strength or hardness. The plastic model (case 1) considering work hardening will be employed to simulate the indentation behavior of the monoclinic ZrO_2.

V. Conclusions

ZrO_2 thin films were deposited on Si substrate by FCVA with different oxygen flow rate. Their mechanical properties (including *E*, *H*, and yield strength (*Y*)) without the substrate effect were then derived by nano-indentation measurement and finite element modeling. Identified by XRD, the structure of the zirconia thin films evolves from amorphous, through pure monoclinic, to amorphous again, with the increase of O_2 flow rate from 10 to 80 sccm. It is found that the elastic-perfect plastic constitutive model is successfully applied to the thin films with amorphous structure; it is however not adequate for the monoclinic ZrO_2, indicating that dislocation related plasticity possibly occurs during nano-indentation examination of the monoclinic ZrO_2. This information indicates that a suitable constitutive model should be adopted for the simulation, providing a guideline for future work.

References

[1]M. J. Paterson, P. J. Paterson, and B. Ben-Nissan, "Dependence of Structural and Mechanical Properties on Film Thickness in Sol-Gel Zirconia Films," *J. Mater. Res.*, **13**, 388–95 (1998).

[2]K. Tanaka, M. Kanari, and N. Matsui, "Continuum Dislocation Model of Vickers Indentation on a Zirconia," *Acta Mater.*, **47**, 2243–57 (1999).

[3]W. C. Oliver and G. M. Pharr, "Improved Technique for Determining Hardness and Elastic Modulus Using Load and Displacement Sensing Indentation Experiments," *J. Mater. Res.*, **7**, 1564–80 (1992).

[4]D. Tabor, *The Hardness of Metal.* London, Oxford, 1951.

[5]S. S. Chiang, D. B. Marshall, and A. G. Evans, "Response of Solids to Elastic/Plastic Indentation-Stresses and Residual Stresses," *J. Appl. Phys.*, **53**, 298–311 (1982).

[6]G. Q. Yu, B. K. Tay, and Z. W. Zhao, "Structure and Properties of Zirconium Oxide Thin Films Prepared by Filtered Cathodic Vacuum Arc," *Appl. Phys. A: Mater. Sci. Process.*, **81**, 405–11 (2005).

[7]S. Xu, B. K. Tay, H. S. Tan, L. Zhong, Y. Q. Tu, S. R. P. Silva, and W. I. Milne, "Properties of Carbon Ion Deposited Tetrahedral Amorphous Carbon Films as a Function of Ion Energy," *J. Appl. Phys.*, **79**, 7234–40 (1996).

[8]J. A. Knapp, D. M. Follstaedt, and S. M. Myers, "Precipitate-Hardened Aluminum Alloys Formed Using Pulsed Laser Deposition," *J. Appl. Phys.*, **79**, 1116–22 (1996).

[9]J. A. Knapp, D. M. Follstaedt, S. M. Myers, J. C. Barbour, and T. A. Friedmann, "Finite-Element Modeling of Nanoindentation," *J. Appl. Phys.*, **85**, 1460–74 (1999).

[10]D. J. Ma, K. W. Xu, and J. W. He, "Numerical Simulation for Determining the Mechanical Properties of Thin Metal Films Using Depth-Sensing Indentation Technique," *Thin Solid Films*, **323**, 183–7 (1998).

[11]*TriboScope User Manual.* Hysitron Inc., Minneapolis, MN, USA, 2002.

[12]Z. H. Gan, Y. B. Zhang, G. Q. Yu, C. M. Tan, S. P. Lau, and B. K. Tay, "Intrinsic Mechanical Properties of Diamond-Like Carbon Thin Films Deposited by Filtered Cathodic Vacuum Arc," *J. Appl. Phys.*, **95**, 3509–15 (2004).

[13]W. B. Li, J. L. Henshall, R. M. Hooper, and K. E. Easterling, "Mechanisms of Indentation Creep," *Acta Metall. Mater.*, **39**, 3099–110 (1991). □